2008/09/29 revised ver.
Journal of Neurophysiology

Organization of color-selective neurons in macaque visual area V4

Yasuyo KOTAKE[1], Hiroshi MORIMOTO[2], Yasutaka OKAZAKI[1],
Ichiro FUJITA[1, 3] and Hiroshi TAMURA[1, 3]

[1] *Laboratory for Cognitive Neuroscience, Graduate School of Frontier Biosciences, and*

[2] *Engineering Science, Osaka University, 1-3 Machikaneyama, Toyonaka, Osaka 560-8531, Japan*

[3] *Core Research for Evolutional Science and Technology (CREST), Japan Science and Technology Agency, Saitama 332-0012, Japan*

Running Head: Organization of color selectivity in V4
Text Pages: 39
Figures & Table: 16 figures, 0 tables

Correspondence to:
Dr. Hiroshi TAMURA
Laboratory for Cognitive Neuroscience, Graduate School of Frontier Biosciences, Osaka University, 1-3 Machikaneyama, Toyonaka, Osaka, 560-8531, Japan
Phone: +81-6-6850-6538
Fax: +81-6-6850-6379
E-mail: tamura@fbs.osaka-u.ac.jp

ABSTRACT

Cortical area V4 in monkeys contains neurons that respond selectively to particular colors. It has been controversial how these color-selective neurons are spatially organized in V4. One view asserts that color-selective neurons are organized in columns with different colors orderly mapped across the cortex, whereas other studies have found no evidence for columnar organization or any other clustered structure. In the present study, we reexamined the functional organization of color-selective neurons in area V4 by quantitatively evaluating and comparing the color selectivity of nearby neurons as well as those encountered along electrode penetrations. Using a multiple single-unit recording technique, we recorded extracellular activities simultaneously from groups of nearby V4 neurons. Color discrimination and color preferences exhibited a moderate correlation between nearby neurons, consistent with neurons in a local region of V4 sharing similar responses to stimulus color. However, the degree of clustering was variable across recording sites. Some regions contained neurons with similar color preferences, while others contained neurons with diverse color preferences. Neurons in penetrations normal to the cortical surface responded to an overlapping range of colors and maintained a moderate correlation. Neurons in penetrations tangential to the cortical surface differed dramatically in their preferred color and exhibited a negative correlation. We conclude that neurons in area V4 are moderately clustered according to their color selectivity, and that this weak clustering is columnar in structure.

INTRODUCTION

Most primates possess well-developed color vision that contributes to the detection of food, predators, and social signals from conspecifics (Changizi et al. 2006; Coss and Ramakrishnan 2000; Dominy 2004; Regan et al. 2001; Waitt et al. 2003). In the visual cortex, color information is processed along the ventral pathway including the striate cortex (V1), the prestriate cortices (V2, V4), and the inferior temporal (IT) cortex (Maunsell and Newsome 1987). Many neurons in these areas convey information about color (Gegenfurtner 2003; Komatsu 1998; Solomon and Lennie 2007).

In V1 and V2, color-selective neurons are clustered in regularly spaced spots or bands across the cortical sheet (Dow 2002; Sincich and Horton 2005). In layers 2 and 3 of V1, color-selective neurons are more abundant in cytochrome oxidase (CO)-rich blobs and narrow strips of cortex bridging blobs than in interblob regions (Landisman and Ts'o 2002; Lu and Roe 2008; Tootell et al. 2004; Ts'o and Gilbert 1988). In V2, color-selective neurons are more frequently encountered in thin CO-stripes than in thick and pale stripes (DeYoe and Van Essen 1985; Hubel and Livingstone 1987; Roe and Ts'o 1995, 1999; Shipp and Zeki 2002; Tootell et al. 2004). Each thin stripe consists of hue- and luminance-preferring domains, and neurons with different hue preferences are segregated within a hue-preferring domain (Roe and Ts'o 1995; Wang et al. 2007; Xiao et al. 2003). However, the degree of clustering of color-selective neurons has otherwise been disputed (Kiper et al. 1997; Leventhal et al. 1995; Tamura et al. 1996).

Organization of color selectivity in V4, a cortical area implicated in color vision in general (Zeki 1980; but see Heywood et al. 1992; Schiller 1993) and color constancy (Walsh et al. 1993; Wild et al. 1985), is even more controversial. Zeki (1973, 1980) proposed that color-selective neurons are

organized in a columnar manner and arranged systematically across the cortex according to their color preferences. A subsequent study reported that V4 neurons are grouped into yellow/achromatic and red/blue columnar clusters of 1-4 mm in width across the cortex (Yoshioka and Dow 1996). Results from Tanaka et al. (1986) did not support the existence of columns for color. Although some of their penetrations in V4 contained only neurons sensitive to long wavelength, they ascribed this finding to the predominance of long-wavelength sensitive neurons. If any of the above organization is present in V4, adjacent neurons should respond to similar colors. However, Schein et al. (1982) found no evidence for similarity in color selectivity between nearby neurons, because only a small fraction of V4 cells in their sample were color selective. These marked discrepancies may have arisen from a combination of several technical factors such as differences in the sampled regions within V4, differences in the definition of color selectivity, sampling bias of recorded neurons, and, predominantly, the qualitative assessment of color selectivity and clustering in preceding studies.

In the present study, we applied a systematic and quantitative analysis to the question of how color-selective neurons are arranged in V4. To minimize possible sampling bias we recorded neural activity with a multiple single-unit recording technique and analyzed the responsiveness of all neurons encountered. We examined responses of neurons to 27 isoluminant colors systematically distributed on the CIE (Commission Internationale de I'Éclairage, 1931) -*xy* chromaticity diagram. We conclude from our quantitative analysis that V4 neurons exhibit a modest degree of columnar clustering for similar color sensitivity and color preference.

METHODS

Animals and initial surgery

Neuronal responses were recorded from area V4 of four hemispheres in three anesthetized monkeys

(*Macaca fuscata*; body weight, 5.2-6.1kg). Recording sites in three hemispheres are shown in Figure 1A-C. General experimental procedures were similar to those described previously (Tamura et al. 2004). An initial surgery was performed at least three weeks before recording experiments. A plastic headpost was implanted on the skull. The surgery was performed under aseptic conditions and full anesthesia by inhalation of 1-3% isoflurane (FORANE, Abbott Japan, Tokyo) in 70% N_2O-30% O_2. An analgesic, ketoprofen (MENAMIN, Chugai, Tokyo), was provided for a week. All procedures for animal care and experimentation were in accordance with the guidelines of the National Institutes of Health (1996) and the Japan Neuroscience Society. The Osaka University Animal Experiment Committee approved the procedures as appropriate and conforming to the current standard of the animal experiment protocols.

Recording of neural activity

The monkeys were first sedated with an injection of atropine sulfate (Tanabe, Osaka; 0.1 mg/kg, i.m.) and ketamine hydrochloride (KETALAR, Daiichi-Sankyo, Tokyo; 12 mg/kg, i.m.), then anesthetized by inhalation of 1-3% isoflurane in 70% N_2O-30% O_2 through an intratracheal cannula. They were held through a head restraint. During the recording session, isoflurane was removed and animals were infused with an opioid agent, fentanyl citrate (FENTANEST, Daiichi-Sankyo, Tokyo; 35 μg/kg/h), and immobilized with pancuronium bromide (MIOBLOCK, Organon Japan, Osaka; 0.02 mg/kg/h) (Popilskis and Kohn 1997). The lactated Ringer's solution with 5% glucose (SOLULACT-D, Terumo, Tokyo) for infusion also contained atropine sulfate (0.01 mg/kg/h), an antibiotic (PENTCILLIN, Toyama Chemical, Toyama, Japan; 0.04 mg/kg/h, i.v.), and riboflavin (BISULASE, Toa Eiyo, Tokyo; 0.8 mg/kg/h, i.v.). The flow rate for infusion was 12 ml/h. Blood pressure, heart rate, arterial oxygen saturation level, and end-tidal CO_2 were monitored throughout the experiment. Body temperature was maintained at 37-38°C. The pupils were dilated and the

lenses were relaxed by applying 0.5% tropicamide-0.5% phenylephrine hydrochloride (MYDRIN-P, Santen, Osaka). The corneas were covered with contact lenses of appropriate refractive power and curvature with an artificial pupil (diameter 3 mm) to focus on a CRT monitor placed 114 cm away.

Multiple single-unit recordings were made from area V4 with a single-shaft electrode with four recording probes (Fig. 1D; "Tetrode", Thomas Recording, Giessen, Germany). The sampling diameter of the electrode was estimated to be at <300 μm (Kaneko et al. 2007). Recordings were made at intervals of ≥300 μm along a penetration, except for the cases specified otherwise, to avoid sampling the same neurons at successive sites. In every vertical penetration, we recorded neuronal activity from the cortical surface to the white matter. All neurons encountered were recorded. Recorded potentials were amplified by x10,000, band-pass filtered (500 to 3000 Hz), digitized at 50-μs resolution, and stored on a computer for off-line analysis. Methods for isolation and classification of spikes from recorded signals have been described elsewhere (Kaneko et al. 1999, 2007; Tamura et al. 2004). Briefly, action potentials (spikes) were detected in recorded signals with an elastic-template matching. Four covariance values between the template and the spikes recorded from four recording sites were vectorized. The vectors were hierarchically clustered using a multidimensional statistical test. Each spike was classified into a cluster and never classified into more than one clusters. Analysis was restricted to units with a total of ≥1000 spikes and not more than 1% of their inter-spike intervals were shorter than 1 ms. In a previous study, we estimated the error rate of our spike sorting method to be at 0.038% (Tamura et al. 2005). This small error rate, i.e., only several erroneous spikes among 10,000 spikes, is unlikely to affect the main conclusions in the present study. In monkey C, one to four small electrolytic lesions were made for each penetration by passing a current of 10 μA for 10 s through the electrode tip to determine the trajectory of the penetrations in subsequent histological analysis (Fig. 1E, F).

********** **Fig. 1 comes near here** **********

After recording, the infusion was switched to lactated Ringer's solution (SOLULACT, Terumo, Tokyo) that contained only atropine sulfate. Spontaneous respiration recovered to normal levels within 1 h after terminating infusion of the muscle relaxant. Recovery was aided by an injection of neostigmine methylsulfate (VAGOSTIGMIN, Shionogi, Osaka; 0.1 mg/kg, i.m.). We rinsed the eyes with saline and administered a drop of antibiotic (TARIVID OPHTHALMIC SOLUTION, Santen, Osaka) and vitamin B_2 (FLAVITAN EYE DROPS, Toa Eiyo, Tokyo). After analgesics and antibiotics were provided, the monkeys were returned to their home cages. Each recording session lasted for 10-15 hr. After one or two weeks of recovery, a next recording experiment was performed. Each monkey was used for 4 to12 months.

Visual stimuli

Color stimuli were generated and controlled by a visual stimulus generator (VSG2/3F, Cambridge Research Systems, Rochester, England) installed on a computer and displayed on a CRT color monitor (FLEXSCAN T965-13K, Eizo Nanao, Ishikawa, Japan) in a bright room. We used 27 isoluminant (33 cd/m^2) colors that were systematically distributed on the CIE-*xy* chromaticity diagram (Fig. 2A). To facilitate comparison of the results in the present study with those in previous studies (e.g., Hanazawa et al. 2000; Kusunoki et al. 2006), the data were plotted on the MacLeod-Boynton chromaticity diagram (Fig. 2B; MacLeod and Boynton 1979). The coordinates of the 27 colors on the MacLeod-Boynton diagram were calculated using the cone spectral sensitivities (Stockman and Sharpe 2000). During the course of the study, the color stimuli were regularly calibrated with a spectrometer (MINOLTA CS-1000, Tokyo, Japan) to reproduce colors properly.

Visual stimuli were drifting square-wave gratings consisting of a stimulus color and black (2.6 cd/m^2, CIE chromaticity coordinate: x = 0.324, y = 0.371) presented on the same black background. This configuration increased stimulus contrast and allowed presentation of a variety of stimulus colors selected from an isoluminant CIE plane. The stationary grating was first flashed for 400 ms before it started to drift in the optimal direction for the multiple units under study. The color of the stimulus for each trial was pseudorandomly selected from the 27 colors. Each color stimulus was presented 10 times to the contralateral eye at the center of the predetermined receptive field (RF) for each recording site.

********** **Fig. 2 comes near here** **********

Experimental protocol

In monkeys A and B, recordings were made at intervals ≥300 μm and only when the recorded signals contained isolatable spikes. In monkey C, we investigated changes in color preferences along electrode penetrations. For this analysis, we recorded at intervals of 125-300 μm; when we did not detect spikes with an amplitude large enough to isolate single units, we used unresolved multiple units (MUs).

At each recording site, we first plotted the location and size of the RF for MUs recorded from the tip probe with a hand-held circular disk, bar, or a grating pattern. The optimal combination of the size, orientation (0° to 180° at 22.5° step), spatial frequency (0.125, 0.25, 0.5, 1, 2, and 4 cycles/degree) and temporal frequency (0.5, 1 and 2 cycles/s) of the stimuli were then determined to identify the stimulus that evoked the maximal response. Here, we assume that color selectivity is separable from other stimulus dimensions. Although we cannot rule out the possibility that preferred color of V4

neurons may depend on other stimulus parameters, a previous study shows that color preference of neurons in the inferior temporal cortex, which receives inputs from V4, is independent from stimulus shape (Komatsu and Ideura 1993).

Histology

After all the experiments were completed, monkeys were deeply anesthetized with an overdose of pentobarbital sodium (100 mg/kg, i.v.) and transcardially perfused with 4% paraformaldehyde (Merck, Darmstadt, Germany). Metal pins were inserted into the brain to verify the recording sites (Fig. 1A-C). In monkey C, the brain was immersed in a graded series of sucrose solutions (10-30%, one week) for histological reconstruction of electrode penetrations. The brain was trimmed, frozen, and cut coronally into 80 μm-thick serial sections. Sections were stained for Nissl substance with cresyl violet. Penetrations and recording sites were reconstructed using the combination of electric lesions and the electrode manipulator readings noted for each recording site (Fig. 1E, F). To evaluate the penetration angle, we measured the angle subtended by the recording track and the columnar array of neurons.

Data analysis

The magnitude of responses was evaluated by calculating the mean spike counts during a 2-s period for drifting gratings. The period for counting spikes was shifted by 120 ms not to include the onset responses. Neurons were considered visually responsive when the firing rates to at least one of the color stimuli differed from the spontaneous firing rate calculated from a time period of 400 ms immediately before stimulus presentation (*t*-test with correction for multiple comparisons; the square root of the firing rate was evaluated; Prince et al. 2002).

To measure the degree of color tuning, we calculated a color discrimination index (CDI). The CDI was determined as follows,

$$\mathrm{CDI} = \frac{R_{\max} - R_{\min}}{R_{\max} - R_{\min} + 2\sqrt{SSE/(N-M)}}$$

where R_{max} and R_{min} are the maximum and minimum responses among the colors tested, *SSE* is the sum of the squared error of the response at each color, *N* is the total number of trials (27 x 10), and *M* is the number of color stimuli tested (27). Note that all of these calculations were performed using the square root of the firing rates without subtracting spontaneous firing rates (Prince et al. 2002). The CDI compares the firing rates between the most preferred and the least preferred colors normalized by the variance across trials. If the responses are stable across stimulus repetitions and consistently different between the most preferred and the least preferred colors, the CDI approaches one. If a neuron is not selective for colors, and the responses do not differ among the tested colors, the index will approach zero. A CDI value of 0.5 indicates that the difference between the maximum response and the minimum response is equal to trial-to-trial response variability.

Neurons were taken as color selective if their firing rates with subtraction of the spontaneous firing rates varied among the isoluminant colors in our stimulus set ($p < 0.05$, Kruskal-Wallis test). For all color-selective neurons, we determined the response field on the MacLeod-Boynton (M-B) chromaticity diagram. We plotted firing rates after subtraction of spontaneous firing rates, and negative values were collapsed to 0. The maximum response color among the 27 colors was first identified. The contours of 75%, 50%, and 25% of the peak response magnitude were determined subsequently by linear interpolation. The area within the color space where stimuli evoked responses greater than 75% of the peak response was defined as the effective color field.

RESULTS

Database

Recordings were made exclusively in the dorsal V4 encompassing the posterior bank of the superior temporal sulcus through the prelunate gyrus (Fig. 1A-C). We recorded the activity of 375 neurons (142, 100, 133 from monkeys A, B, C, respectively) from 109 sites (34 from monkey A, 22 from monkey B, 53 from monkey C). Multiple single-unit recording enabled us to isolate up to 13 neurons (median, 3) at a single recording site. Among the 375 neurons examined, 282 (75%) from 74 sites responded to at least one of the stimuli tested ($p < 0.05$, *t*-test corrected for multiple comparisons). The RF centers were located in the contralateral, lower visual field or around the horizontal meridian, 0.3 - 4.3° (Monkeys A and B) or 0.2 - 11.5° (Monkey C) from the fovea.

Color-selective responses of V4 neurons

A majority of the visually responsive V4 neurons (65%, 182/282) displayed a color preference ($p < 0.05$, Kruskal-Wallis test). Figure 3 shows peristimulus time histograms (PSTHs) on the CIE-*xy* color space (upper panels) and bubble plots on the MacLeod-Boynton (M-B) diagram (lower panels) for the responses of four representative color-selective neurons. The neuron in Figure 3A responded to khaki, red, and orange (e.g., colors 3-5, 9, 12), but not to the other colors. The color discrimination index (CDI, see Methods) of this neuron was 0.72. Thus, this neuron reliably discriminated the optimal color from the least-preferred color. The firing rate of the neuron in Figure 3B increased in response to blue stimuli (colors 22, 25) and decreased in response to red and magenta stimuli (colors 5, 9, 18). The CDI of this neuron was 0.65. Both of these neurons responded to colors on the edge of the chromaticity diagrams, preferring saturated colors to unsaturated ones. In contrast, the neuron in Figure 3C responded to unsaturated colors (colors 14, 17) in the center of the color space (CDI = 0.68). The neuron in Figure 3D represents a smaller group of neurons that

responded to two distinct groups of colors, khaki and violet (CDI = 0.68).

********** **Fig. 3 comes near here** **********

The CDIs were distributed unimodally in each monkey (Hartigan's dip test, $p = 0.56$ for monkey A, $p = 0.44$ for monkey B, $p = 0.98$ for monkey C; Fig. 4). The median CDIs were 0.51, 0.52 and 0.45 for monkeys A-C, respectively, and 0.49 for the combined data. The distribution of CDIs was different among the three monkeys ($p < 0.001$, Kruskal-Wallis test). CDIs for monkey C were lower than those for monkey B ($p = 0.002$, Mann-Whitney U-test), but were not different from those of monkey A ($p = 0.12$, Mann-Whitney U-test). As recordings from monkey C included neurons with more peripheral RFs (~11.5°) than those in monkey B (~3.2°), we examined if there was any difference in CDIs between neurons having RFs in a parafoveal region (eccentricity ≤ 3.2°) and those having RFs in a peripheral region (eccentricity > 3.2°) in monkey C. We did not find any difference in CDIs between them ($p = 0.32$, Mann-Whitney U-test). In addition, the CDI values were not correlated with the eccentricity of RFs in monkey C (Spearman's rank correlation coefficient, $r = -0.003$, $p = 0.98$).

********** **Fig. 4 comes near here** **********

Color response fields of V4 neurons

The preferred color stimulus for V4 neurons differed across neurons. The number of color stimuli that evoked maximal responses in at least one neuron was 21 (78% of the color stimuli) on average across monkeys. In other words, the remaining stimuli did not evoke maximal responses in any neuron. Preferred colors were not evenly distributed over the color space (Fig. 5). Approximately

80% of neurons tested responded optimally to colors on the edge of the color space and thus preferred more saturated colors to less saturated ones. As has been reported previously (Schein et al. 1982; Tanaka et al. 1986), more neurons preferred red colors to other saturated colors such as blue and violet.

********** **Fig. 5 comes near here** **********

Among the 182 color-selective neurons, 109 (60%) had a single peak, 58 (32%) had two peaks and 15 (8%) had three or four peaks in the color space. No neuron had more than four peaks. To gauge how neurons combined cone inputs, we classified 109 neurons with a single peak according to the criteria of Hanazawa et al. (2000). No neurons in our sample belonged to Type 1, which had approximately linear contours with an equal spacing on the M-B chromaticity diagram. Nine percent of neurons with a single peak were Type 2, which also had approximately liner contours with its effective stimuli confined within the color space (Fig. 6A, B). Type 3 and 4 neurons had curved contours. The response peak of Type 3 neurons was located at the periphery of the color space (Fig. 6C), while that of Type 4 neurons was located in the center of the color space (Fig. 6D). Type 3 and 4 neurons comprised 73% and 17% of the neurons with a single peak, respectively. Type 4 neurons have been found in V1 and IT, but not in the parvocellular layer of the lateral geniculate nucleus (Hanazawa et al. 2000). Therefore the way in which cone inputs are combined in V4 is similar to that in V1 and IT (Hanazawa et al. 2000; Komatsu et al. 1992; Kusunoki et al. 2006).

Type 4 neurons may be tuned for low saturation colors. Alternatively, they may be better viewed as neurons tuned for a circumscribed region in the color space which happened to be in the center of the color space. Stronger evidence for tuning for saturation per se would be neurons that have an annular

tuning profile in a 2-dimensional color space. This kind of neurons has been found in the inferior temporal cortex (see Fig. 7D of Komatsu et al., 1992). We found no such neurons in our V4 sample.

The extent of the effective color field (the color stimulus area where stimuli evoke reponses greater than 75% of the optimal response) differed between neurons (Fig. 6), ranging from 0.1 to 61% (0.1-17% for monkey A; 0.1-61% for monkey B; 0.6-25% for monkey C). The median area of the effective color filed was 2.0% for monkey A, 2.9% for monkey B and 3.9% for monkey C. V4 neurons are highly tuned to a circumscribed region in the color space.

********** **Fig. 6 comes near here** **********

We superimposed the effective color field for each of the sampled neurons to obtain the effective color field for a neuron population in each monkey. The extent of the effective color field of a population of V4 neurons differed among monkeys (68% in monkey A, 92% in monkey B, 89% in monkey C). Whereas most of the color-selective V4 neurons in monkey A preferred highly saturated colors and their effective color field occupied only the periphery of color space (Fig. 7A), the effective color field for monkey B and C extended into the center of color space (Fig. 7B, C) and covered the entire color space.

********** **Fig. 7 comes near here** **********

Clustering of color-selective neurons in V4

Thus, the degree of color discrimination, the optimal color, and the extent of the color field varied among V4 neurons (Figs. 3-6). Next we examined whether neighboring V4 neurons shared color

discrimination, the extent of the effective color field, and color preference. We compared the CDIs between pairs of nearby neurons simultaneously recorded at a given site. This analysis included a total of 54 sites where two or more responsive neurons were recorded. These sites contained 704 neuron pairs derived from 255 neurons, including both neurons that were color-selective as well as those that were nonselective (99 from monkey A; 74 from monkey B; 82 from monkey C). The CDI values were positively correlated between nearby neurons in all the three monkeys (Spearman's rank correlation coefficient $r = 0.38$, $p < 0.001$; Fig. 8).

In Figure 8, the CDI value from a neuron in a pair was arbitrarily allocated to either the abscissa or the ordinate and that of the other neuron was allocated to the other axis. It is conceivable, although unlikely, that the correlation coefficient we obtained (0.38) might be specific for this particular assignment condition. To evaluate how well the results in Figure 8 represented similarity in the CDI values between adjacent neurons, we repeated the same analysis 5000 times by randomly changing assignment of each neuron in a pair to either the abscissa or the ordinate. Note that we fixed neuron-pairs and changed only the assignment of each neuron of a pair to the horizontal or vertical axis.; we did not randomly pair two neurons recorded at different sites. The median of the recalculated 5,000 correlation coefficients was 0.37, a value similar to that obtained in Figure 8. When the correlation coefficient of CDIs was calculated for artificially generated neuron pairs from the same database excluding neighboring neuron pairs (i.e., the coefficient between pairs of distant neurons), it was –0.005 ($p = 0.500$, $n = 31681$). We conclude from these results that nearby neurons had similar color discrimination ability. We also examined the correlation of the extent of effective color filed, which represent sharpness of color tuning. It was not correlated between nearby neurons, indicating that they did not share the degree of tuning.

********** Fig. 8 comes near here **********

We next selected color-selective neurons ($p < 0.05$, Kruskal-Wallis test) from our sample and examined whether they are clustered by color preference. We analyzed 345 pairs of neighboring color-selective neurons obtained from 156 neurons at 38 sites from which two or more color-selective neurons were recorded (58 neurons from monkey A, 58 neurons from monkey B, 40 neurons from monkey C). One representative pair shown in Figure 9A responded to red colors (colors 4, 5, 9, 12), and their overall response profiles were highly similar (Spearman's rank correlation coefficient $r = 0.91$, $p < 0.001$). Another pair responded maximally to an unsaturated color (color 17) and blue (color 25); their response profiles were also strongly correlated ($r = 0.76$, $p < 0.001$; Fig. 9B). However, some pairs were independent or even displayed negative correlations in their color preferences. Response profiles of the pair shown in Figure 9C were independent ($r = 0.19$, $p = 0.35$), while in the pair shown in Figure 9D they were negatively correlated ($r = -0.81$, $p < 0.001$).

********** Fig. 9 comes near here **********

The distribution of correlation coefficients between neighboring neurons was shifted toward positive values with the medians of 0.17-0.29 for the three monkeys. These values were significantly different from zero ($p \leq 0.001$ for all the three monkeys, Wilcoxon's signed-rank test; Fig. 10A). Among the 345 pairs, 110 pairs (32%) displayed a significant positive correlation ($p < 0.05$), whereas a significant negative correlation was observed only in 27 pairs (8%). This overall positive correlation is not simply a reflection of the population bias in color preference of V4 neurons (Figs. 5, 7), because the correlation coefficient calculated from artificially resampled pairs from the same

database excluding neighboring neuron pairs (i.e., the coefficient between pairs of distant neurons) was not different from zero (median, -0.004 to 0.08 for the three monkeys; $p > 0.05$, Wilcoxon's signed-rank test; Fig. 10B). Furthermore, the correlation coefficients of pairs of nearby neurons were greater than that of pairs of neurons spaced farther apart ($p < 0.001$ for each monkey, Mann-Whitney U-test; Fig. 10). We conclude that nearby color-selective neurons share preferred color to a modest degree.

********** **Fig. 10 comes near here** **********

The broad distribution of correlation coefficients (Fig. 10) can be accounted for by two different spatial arrangements of color selective neurons. In one model, each local region in V4 contains neuron pairs with varying degrees of similarity in color preference; i.e., correlation coefficients are broadly distributed even at a single site. Alternatively, clusters of neurons may display more similar color selectivity at some sites but less similarity at other sites. To discriminate between these two possibilities, we evaluated the variability of color correlation coefficients at each recording site (Fig. 11A-C). For this analysis we chose a total of 27 sites where three or more color-selective neuronal pairs were recorded. Some sites contained pairs with similar correlation coefficients and standard deviations (SDs) of the values were small. At these sites, most neuronal pairs exhibited positive correlation coefficients (Fig. 11D). At other sites, we found pairs with high positive correlation as well as pairs with negative correlation (Fig. 11E). These sites showed a large SD of the correlation coefficient. Across recording sites, the SDs were not correlated with the number of neurons recorded at a single site ($r = 0.33$, $p = 0.35$, for monkey A; $r = 0.15$, $p = 0.72$, for monkey B; $r = 0.41$, $p = 0.33$ for monkey C; Spearman's rank correlation coefficient). We conclude from these findings that the degree of similarity in color preferences differs among different local regions. Some regions

comprise neurons with similar color preferences, whereas other regions consist of neurons with more diverse color preferences

********** **Fig. 11 comes near here** **********

Color selectivity along electrode penetrations

Last, we addressed whether the modest but significant clustering of color selectivity is a consequence of columnar organization. We analyzed the color preference of neurons along electrode penetrations that traversed V4 at various angles to the cortical surface. We reconstructed 11 penetrations histologically by identifying electrolytic lesions made during the recording sessions. In eight penetrations, color-selective neurons (56 neurons) or unresolved multiple units (9 MUs) were recorded at two or more recording sites.

Among the 11 histologically reconstructed penetrations, nine were vertical (≤10º between the electrode path and the radial array of cortical neurons) or near-vertical penetrations (15-30 º degrees). Based on the fraction of color selective neurons, the 9 vertical or near-vertical penetrations were grouped into two types. In 6 of the 9 penetrations, 50-80% of the recorded neurons were selective for color, whereas in the remaining 3 penetrations only 20-38% of the recorded neurons were color-selective. The average CDI value for the 6 penetrations of a higher proportion of color-selective neurons (0.48) was slightly higher than that of the 3 penetrations (0.41; $p < 0.001$, Mann-Whitney U-test). One of the three penetrations was close to the lunate sulcus, and another was close to the dorsal tip of the inferior occipital sulcus, and yet another was located at the center of the prelunate gyrus. The remaining 2 penetrations included, on average, 22.5% of color neurons. One of the two penetrations was close to the lunate sulcus, and the other

was located at the center of the prelunate gyrus. We thus did not find any clear-cut difference in the spatial distribution between penetrations with a high proportion of color-selective neurons and those with a low proportion of color-selective neurons.

Figure 12 shows the results from a penetration perpendicular to the cortical surface. Histological reconstruction revealed that the angle between the electrode path and the radial array of neurons was 2° (Fig. 12A). The six recording sites spanned 1400 μm across the gray matter. RF centers of the MUs recorded at these sites were all located near the fovea, and the RF centers shifted only by less than 1.0º in eccentricity as we advanced the electrode (Fig. 12B). Along this penetration, we obtained 22 visually responsive neurons at six recording sites. Among the 22 neurons examined, 17 (77%) were selective for color ($p < 0.05$, Kruskal-Wallis test; Fig. 12C). Most of these neurons responded to red and khaki colors, whereas a few neurons preferred unsaturated colors, blue or green (Fig. 12C). The effective color fields of the 17 color neurons, when combined, occupied 51% of the M-B diagram.

We evaluated how color correlation coefficients changed as a function of distance between the recorded neurons. The median coefficient for all the recording pairs excluding those recorded with a distance of less than 300 μm was significantly larger than zero (median = 0.25, $p \fallingdotseq 0.002$, Wilcoxon's signed-rank test; Fig. 12D), although the color correlation coefficients were widely distributed and the median coefficient slightly declined for larger distances. The median of correlation coefficient between neuron pairs recorded at single sites (38 neuron pairs) and adjacent sites (200-235 μm, 20 neuron pairs) was 0.26 and 0.46, respectively. These two correlation coefficients were not significantly different from each other ($p < 0.05$, Mann-Whitney U-test). Neurons thus maintained a modest degree of similarity in color preference throughout this

penetration. We further addressed if there was a slow and systematic shift in preferred color along this penetration by examining whether the physical distance between two neurons along the penetration was correlated with the distance between preferred colors on the M-B diagram. We found no correlation between them ($r = 0.03$, $p = 0.70$, Spearman's rank correlation coefficient).

********** **Fig. 12 comes near here** **********

Figure 13 illustrates data from another penetration perpendicular to the cortical surface. The angle between the electrode path and the radial array of cells above layer 4 was 3°, whereas it was 30º in the infragranular layer because of the complex sulcal structure beneath the gray matter (Fig. 13A). Thus, this penetration was normal to the cortex only in the superficial layers that contained recording sites 1 to 4. Shifts in eccentricity of RF centers ranged from 0.8 to 1.1º for MUs at the 7 sites (Fig. 13B). Among 7 neurons recorded at the first 4 sites, 6 (86%) were selective for color ($p < 0.05$). All these six neurons preferred unsaturated colors near the top of the M-B diagram (colors, 7, 11, 14) or blue (color 19). The effective color fields of the 6 neurons combined covered 49% of the M-B diagram. When we advanced the electrode into the infragranular layers (sites 5-7), where the electrode track was no longer parallel to the neuronal arrays, the preferred colors jumped from unsaturated (color 17, site 6) to khaki (color 4, site 7).

The distribution of color correlation coefficients obtained from neuron pairs in the superficial layers, except for the neuron pairs from the same site, was significantly deviated from zero (median = 0.30, $p = 0.001$, Wilcoxon's signed-rank test; Filled circle in Fig. 13D). When we included neurons in the infragranular layers, the distribution of color correlation coefficients was not deviated from zero (median = 0.07, $p = 0.59$, Wilcoxon's signed-rank test; Filled diamond in Fig. 13D). In the

superficial layers, the distance between preferred colors on the M-B diagram was not correlated with the recording-site distance (r = 0.22, p = 0.43, Spearman's rank correlation coefficient), suggesting no slow and systematic shift in preferred color along this penetration.

********** **Fig. 13 comes near here** **********

To address what proportions of penetrations is necessary in Monkey C to produce a given coverage of the color field, we calculated the effective color field for a neuron population by superimposing the effective color field for neurons recorded in a single vertical penetration. The area was 33% on average across 5 vertical penetrations ≤10° between the electrode path and the radial array of cortical neurons; Fig. 14). In 3 penetrations with a higher CDI, the area was 48%. The results indicate that neurons obtained in a single penetration can be activated by color stimuli in 30-50% of the M-B diagram.

Next, we examined relation between the number of perpendicular penetrations pooled for calculation of population effective color field and the area of the combined field. As we increased the number of penetrations pooled, the covered area gradually increased (Fig. 14). With the 5 perpendicular penetrations pooled, the coverage of effective color field was 70%. The results suggest that a single local site in V4 is not enough la to achieve a high degree of color coverage.

********** **Fig. 14 comes near here** **********

The penetration shown in Figure 15 is an example of an oblique/tangential penetration. The electrode penetrated the supragranular layers with an angle of 50-90° between the electrode path and

radial array of cells (Fig. 15A). The angle changed drastically along the track because the penetration was made at the shoulder of the superior temporal sulcus. Along this penetration, we obtained seven color-selective units (five single units and two MUs). The eccentricity of RF centers changed by 2º with advancement of the electrode (Fig. 15B). The preferred colors changed rapidly with electrode advancement. For the first two sites (sites 2 and 4), preferred colors were orange (colors 12, 15; Fig. 15C). Three of the five neurons recorded at the next site (site 5) preferred green and bluish green (colors 10, 13), while the other two neurons responded best to magenta and violet (colors 18, 23). The overall distribution of correlation coefficients (11 neuron pairs), excluding the data at the same site, shifted toward negative values and differed from zero (median = -0.28, $p = 0.028$, Wilcoxon's signed-rank test; Fig. 15D), while the median color correlation coefficient between neurons at the same site (10 neuron pairs) was 0.18. We conclude from these results that the rate of change of preferred color along this oblique penetration was more rapid than in the vertical penetrations shown in Figures 12 and 13.

********** **Fig. 15 comes near here** **********

We then quantified relationship between the distance of two neurons along the cortical sheet and their color correlation coefficient. Color correlation coefficient was negatively correlated with the tangential distance ($r = -0.11$, $p = 0.049$, Spearman's rank correlation coefficient; Fig. 16); neuron pairs with a shorter tangential distance exhibited higher color correlation coefficients than those with a longer distance. This relationship was not observed between the normal distance and color correlation coefficient ($r = 0.005$, $p = 0.93$).

********** **Fig. 16 comes near here** **********

DISCUSSION

Understanding of how neurons with selectivity for various stimuli are spatially arranged within a brain region provides clues to information processing, input/output organization, and development (Cohen and Knudsen 1999; Fujita 2002; Hubel and Wiesel 1977; Nelson and Bower 1990, Purves et al. 1992). Though it may appear straightforward, determining the spatial arrangement of neuronal selectivity often suffers from various technical confounds. By employing multiple single-unit recording and quantitative assessment of color selectivity, we revisited a long-lasting, controversial aspect of the organization of color-selective neurons in area V4. We demonstrate that nearby neurons exhibited similar color discrimination and shared color preferences. The degree of similarity in color preferences was modest on average and differed among recording sites. Sequential recordings along penetrations revealed that color preferences changed more slowly in normal penetrations than in oblique penetrations. Thus, V4 neurons are moderately clustered in a columnar manner according to their color sensitivity and selectivity.

Color selectivity of V4 neurons

Using multiple single-unit recordings, we sampled all neurons that could be isolated at regular intervals across cortical layers. Our sampling did not involve any selection criteria other than responsiveness to the visual stimuli. The stimulus gratings comprised black portions and colored portions that were isoluminant but varied in hue and saturation. A large majority (65%) of the neurons responsive to this stimulus set differentially responded to different isoluminant colors. The median CDI was 0.49, indicating that the modulation amplitude by different colors equaled the averaged trial-by-trial variation in responses by typical V4 neurons. The amplitude of response modulation by color was similar to values reported for binocular disparity modulation for V4

neurons (median disparity discrimination index = 0.48; Tanabe et al. 2005).

Most previous studies have used monochromatic stimuli (Schein et al. 1982; Tanaka et al. 1986; Zeki 1973) or color stimuli at different luminance (Yoshioka et al. 1996; Yoshioka and Dow 1996). Monochromatic stimuli only probe selectivity for hue. Because some neurons in V1 are selective for a combination of hue and saturation (Hanazawa et al. 2000), full characterization of color selectivity of V4 neurons requires a stimulus set covering a significant volume of the color space.

Spatial organization of color selectivity in V4

The CDI values were correlated between nearby neurons, but not between distant neurons. Therefore, V4 neurons are clustered according to their ability of color discrimination. The distribution of CDI values was unimodal, consistent with the model that color-selective clusters and non-color selective clusters are not distinct entities but response properties that gradually transit from one to the other across cortex. An earlier study reported that color-selective neurons are more often found in a posterior portion of V4 (i.e., the anterior bank of the lunate sulcus) than in other regions (Zeki 1983). Results from recent studies employing 2-deoxy-glucose mapping, functional magnetic resonance imaging (fMRI), or intrinsic optical signal imaging are consistent with this observation that strongly color-biased responses are present in a posterior portion of the prelunate gyrus (Conway and Tsao 2006; Tanigawa et al. 2007; Tootell et al. 2004).

Conway et al. (2007) reported that color-biased hotspots in fMRI data avoid the crest of the prelunate gyrus. They suggest that neurons in the bank of the lunate sulcus are color-tuned, whereas those in the prelunate gyrus part of V4 are not. Our recordings were performed mostly in the prelunate gyrus, yet 65% of visually responsive neurons were color-selective by our criteria.

However, the color selectivity of most V4 neurons is only modest (median CDI = 0.49). This response modulation may be difficult to detect by comparing responses to chromatic and achromatic stimuli with fMRI techniques. It is likely that only regions clustered with neurons of a high CDI may be evident as color-selective spots while other color-selective areas with smaller CDIs may not be detectable. We did find that some penetrations contained a higher fraction of color-selective neurons than in other penetrations. Another technical confound is that Conway et al. (2007) used full-field visual stimuli. V4 neurons are strongly inhibited by stimuli outside the RF (Desimone and Schein 1987), and are not optimally responsive to a large, full-field stimulus.

The degree of clustering of neurons with similar color preferences differed across recording sites (Fig. 11). This result may reflect heterogeneity of the degree of clustering of neurons with similar color preference within V4. An alternative interpretation is that clusters of V4 neurons with different color preferences may abut at occasional singularity points, similar to the manner in which columns of neurons with different orientation preferences meet at ‘pinwheel centers’ in V1 (Dow 2002). Notionally, recording from these singular points would yield clusters of neurons with larger variances in their preferred colors than clusters of neurons in other regions.

In addition to color, V4 neurons convey information about shape, shading, grating pattern, and binocular disparity (Desimone and Schein 1987; Gallant et al. 1996; Hinkle and Connor 2001; Hanazawa and Komatsu 2001; Kobatake and Tanaka 1994; Watanabe et al. 2002; Zeki 1973, 1983). Neighboring V4 neurons display similar selectivity for non-Cartesian gratings (Gallant et al. 1996) and for binocular disparity (Tanabe et al. 2005; Watanabe et al., 2002). Similarly, neurons in cytoarchitectonic area TE of the inferior temporal cortex, the next stage in the ventral pathway, are tuned to various stimulus attributes including shape, shading, color, and binocular disparity, and are

clustered according to their selectivity for shape and shading (Fujita et al. 1992; Gawne and Richmond 1993; Tamura et al. 2005; Wang et al. 2000) as well as for binocular disparity (Yoshiyama et al. 2004). The degree of clustering is only modest for each of these stimulus modalities in V4 and TE compared to area MT where nearby neurons display strongly correlated motion direction preference and binocular disparity selectivity (Albright et al. 1984; DeAngelis and Newsome 1999). It is unclear both how this information for different modalities is combined at the single neuron level in V4 and TE, and how neurons selective for different modalities are organized. Applying 2-photon calcium imaging techniques *in vivo* may help reveal the detailed functional architecture of these areas.

ACKNOWLEDGMENTS

We thank Makoto Kusunoki and Akitoshi Hanazawa for comments on the manuscript, Hidekazu Kaneko for help with spike sorting, Yoshiya Mori and Tatsuo Nishiki for technical assistance.

GRANTS

This work was supported by grants from Core Research for Evolutional Science and Technology of the Japan Science and Technology Corporation (IF) and from the Ministry of Education, Culture, Sports, Science and Technology of Japan (IF, HT).

REFERENCES

Albright TD, Desimone R, and Gross CG. Columnar organization of directionally selective cells in visual area MT of the macaque. *J Neurophysiol* 51:16-31, 1984.

Changizi MA, Zhang Q, and Shimojo S. Bare skin, blood and the evolution of primate colour vision. *Biol Lett* 2:217-221, 2006.

Cohen YE and Knudsen EI. Maps versus clusters: different representations of auditory space in the midbrain and forebrain. *Trends Neurosci* 22:128-135, 1999.

Conway BR, Moeller S, and Tsao DY. Specialized color modules in macaque exstrastriate cortex. *Neuron* 56:560-573, 2007.

Conway BR and Tsao DY. Color architecture in alert macaque cortex revealed by FMRI**.** *Cereb Cortex* 16:1604-1613, 2006.

Coss RG and Ramakrishnan U. Perceptual aspects of leopard recognition by wild bonnet macaques (*Macaca radiata*). *Behaviour* 137:315-335, 2000.

DeAngelis GC and Newsome WT. Organization of disparity-selective neurons in macaque area MT. *J Neurosci* 19:1398-1415, 1999.

Desimone R and Schein SJ. Visual properties of neurons in area V4 of the macaque: sensitivity to stimulus form. *J Neurophysiol* 57:835-868, 1987.

DeYoe EA and Van Essen DC. Segregation of efferent connections and receptive field properties in visual area V2 of the macaque. *Nature* 317:58-61, 1985.

Dominy NJ. Fruits, fingers, and fermentation: The sensory cues available to foraging primates. *Integr Comp Biol* 44:295-303, 2004.

Dow BM. Orientation and color columns in monkey visual cortex. *Cereb Cortex* 12:1005-1015, 2002.

Fujita I. The inferior temporal cortex: architecture, computation, and representation. *J Neurocytol*

31:359-371, 2002.

Fujita I, Tanaka K, Ito M, and Cheng K. Columns for visual features of objects in monkey inferotemporal cortex. *Nature* 360:343-346, 1992.

Gallant JL, Connor CE, Rakshit S, Lewis JW, and Van Essen DC. Neural responses to polar, hyperbolic, and Cartesian gratings in area V4 of the macaque monkey. *J Neurophysiol*. 76: 2718-2739, 1996.

Gawne TJ and Richmond BJ. How independent are the messages carried by adjacent inferior temporal cortical neurons? *J Neurosci* 13:2758-2771, 1993.

Gegenfurtner KR. Cortical mechanisms of colour vision. *Nat Rev Neurosci*. 4:563-572, 2003.

Hanazawa A and Komatsu H. Influence of the direction of elemental luminance gradients on the responses of V4 cells to textured surfaces. *J Neurosci* 21:4490-4497, 2001.

Hanazawa A, Komatsu H, and Murakami I. Neural selectivity for hue and saturation of colour in the primary visual cortex of the monkey. *Eur J Neurosci* 12:1753-1763, 2000.

Heywood CA, Gadotti A, and Cowey A. Cortical area V4 and its role in the perception of color. *J Neurosci* 12:4056-4065, 1992.

Hinkle DA and Connor CE. Disparity tuning in macaque area V4. *Neuroreport* 12:365-369, 2001.

Hubel DH and Wiesel TN. Ferrier lecture. Functional architecture of macaque monkey visual cortex. *Proc R Soc Lond B Biol Sci* 198:1-59, 1977.

Hubel DH and Livingstone MS. Segregation of form, color, and stereopsis in primate area 18. *J Neurosci* 7:3378-3415, 1987.

Kaneko H, Suzuki SS, Okada J, and Akamatsu M. Multineuronal spike classification based on multisite electrode recording, whole-waveform analysis, and hierarchical clustering. *IEEE Trans Biomed Eng* 46:280-290, 1999.

Kaneko H, Tamura H, and Suzuki SS. Tracking spike-amplitude changes to improve the quality of

multineuronal data analysis. *IEEE Trans Biomed Eng* 54:262-272, 2007.

Kiper DC, Fenstemaker SB, and Gegenfurtner KR. Chromatic properties of neurons in macaque area V2. *Vis Neurosci* 14:1061-1072, 1997.

Kobatake E and Tanaka K. Neuronal selectivities to complex object features in the ventral visual pathway of the macaque cerebral cortex. *J Neurophysiol* 71:856-867, 1994.

Komatsu H. Mechanisms of central color vision. *Curr Opin Neurobiol* 8:503-508, 1998.

Komatsu H and Ideura Y. Relationships between color, shape, and pattern selectivities of neurons in the inferior temporal cortex of the monkey. *J Neurophysiol* 70:677-694, 1993.

Komatsu H, Ideura Y, Kaji S, and Yamane S. Color selectivity of neurons in the inferior temporal cortex of the awake macaque monkey. *J Neurosci* 12:408-424, 1992.

Kusunoki M, Moutoussis K, and Zeki S. Effect of background colors on the tuning of color-selective cells in monkey area V4. *J Neurophysiol* 95:3047-3059, 2006.

Landisman CE and Ts'o DY. Color processing in macaque striate cortex: relationships to ocular dominance, cytochrome oxidase, and orientation. *J Neurophysiol* 87:3126-3137, 2002.

Leventhal AG, Thompson KG, Liu D, Zhou Y, and Ault SJ. Concomitant sensitivity to orientation, direction, and color of cells in layers 2, 3, and 4 of monkey striate cortex. *J Neurosci* 15:1808-1818, 1995.

Lu HD and Roe AW. Functional organization of color domains in V1 and V2 of macaque monkey revealed by optical imaging. *Cereb Cortex* 18:516-533, 2008.

MacLeod DI and Boynton RM. Chromaticity diagram showing cone excitation by stimuli of equal luminance. *J Opt Soc Am* 69:1183-1186, 1979.

Maunsell JH and Newsome WT. Visual processing in monkey extrastriate cortex. *Annu Rev Neurosci* 10:363-401, 1987.

Nelson ME and Bower JM. Brain maps and parallel computers. *Trends Neurosci* 13:403-408, 1990.

Popilskis SJ and Kohn DF. Anesthesia and analgesia in nonhuman primates. In: *Anesthesia and analgesia in laboratory animals.* (Kohn DF, Wixson SK, White WJ, and Benson GJ, eds.) Academic Press, New York. NY; P233-P255, 1997.

Prince SJ, Pointon AD, Cumming BG, and Parker AJ. Quantitative analysis of the responses of V1 neurons to horizontal disparity in dynamic random-dot stereograms. *J Neurophysiol* 87:191-208, 2002.

Purves D, Riddle DR, and LaMantia AS. Iterated patterns of brain circuitry (or how the cortex gets its spots). *Trends Neurosci* 15:362-368, 1992.

Regan BC, Julliot C, Simmen B, Viénot F, Charles-Dominique P, and Mollon JD. Fruits, foliage and the evolution of primate colour vision. *Phil Trans R Soc Lond B Biol Sci* 356:229-283, 2001.

Roe AW and Ts'o DY. Visual topography in primate V2: multiple representation across functional stripes. *J Neurosci* 15:3689-3715, 1995.

Roe AW and Ts'o DY. Specificity of color connectivity between primate V1 and V2. *J Neurophysiol* 82:2719-2730, 1999.

Schein SJ and Desimone R. Spectral properties of V4 neurons in the macaque. *J Neurosci* 10:3369-3389, 1990.

Schein SJ, Marrocco RT, and de Monasterio FM. Is there a high concentration of color-selective cells in area V4 of monkey visual cortex? *J Neurophysiol* 47:193-213, 1982.

Schiller PH. The effects of V4 and middle temporal (MT) area lesions on visual performance in the rhesus monkey. *Vis Neurosci* 10:717-746, 1993.

Shipp S and Zeki S. The functional organization of area V2, I: specialization across stripes and layers. *Vis Neurosci* 19:187-210, 2002.

Sincich LC and Horton JC. The circuitry of V1 and V2: integration of color, form, and motion.

Annu Rev Neurosci 28:303-326, 2005.

Solomon SG and Lennie P. The machinery of colour vision. *Nat Rev Neurosci* 8:276-286, 2007.

Stockman A and Sharpe LT. Tritanopic color matches and the middle- and long-wavelength-sensitive cone spectral sensitivities. *Vision Res* 40:1739-1750, 2000.

Tamura H, Kaneko H, and Fujita I. Quantitative analysis of functional clustering of neurons in the macaque inferior temporal cortex. *Neurosci Res* 52:311-322, 2005.

Tamura H, Kaneko H, Kawasaki K, and Fujita I. Presumed inhibitory neurons in the macaque inferior temporal cortex: visual response properties and functional interactions with adjacent neurons. *J Neurophysiol* 91:2782-2796, 2004.

Tamura H, Sato H, Katsuyama N, Hata Y, and Tsumoto T. Less segregated processing of visual information in V2 than in V1 of the monkey visual cortex. *Eur J Neurosci* 8:300-309, 1996.

Tanabe S, Doi T, Umeda K, and Fujita I. Disparity-tuning characteristics of neuronal responses to dynamic random-dot stereograms in macaque visual area V4. *J Neurophysiol* 94:2683-2699, 2005.

Tanaka M, Weber H, and Creutzfeldt OD. Visual properties and spatial distribution of neurones in the visual association area on the prelunate gyrus of the awake monkey. *Exp Brain Res* 65:11-37, 1986.

Tanigawa H, Lu HD, Chen G, and Roe AW. Functional organization of foveal V4 revealed by optical imaging in the behaving macaque monkey. *Soc Neurosci Abstr* 122.4, 2007.

Tootell RBH, Nelissen K, Vanduffel W, and Orban, GA. Search for color 'center(s)' in macaque visual cortex. *Cereb Cortex* 14:353-363, 2004.

Ts'o DY, Frostig RD, Lieke EE, and Grinvald A. Functional organization of primate visual cortex revealed by high resolution optical imaging. *Science* 249:417-420, 1990.

Ts'o DY and Gilbert CD. The organization of chromatic and spatial interactions in the primate

striate cortex. *J Neurosci* 8:1712-1727, 1988.

Waitt C, Little AC, Wolfensohn S, Honess P, Brown AP, Buchanan-Smith HM, and Perrett DI. Evidence from rhesus macaques suggests that male coloration plays a role in female primate mate choice. *Proc Bio Sci* 270:S144-S146, 2003.

Walsh V, Carden D, Butler SR, and Kulikowski JJ. The effects of V4 lesions on the visual abilities of macaques: hue discrimination and colour constancy. *Behav Brain Res* 53:51-62, 1993.

Wang Y, Fujita I, and Murayama Y. Neuronal mechanisms of selectivity for object features revealed by blocking inhibition in inferotemporal cortex. *Nat Neurosci* 3:807-813, 2000.

Wang Y, Xiao Y, and Felleman DJ. V2 thin stripes contain spatially organized representations of achromatic luminance change. *Cereb Cortex* 17:116-129, 2007.

Watanabe M, Tanaka H, Uka T, and Fujita I. Disparity-selective neurons in area V4 of macaque monkeys. *J Neurophysiol 8*7:1960-1973, 2002.

Wild HM, Butler SR, Carden D, and Kulikowski JJ. Primate cortical area V4 important for colour constancy but not wavelength discrimination. *Nature* 313:133-135, 1985.

Xiao Y, Wang Y, and Felleman DJ. A spatially organized representation of colour in macaque cortical area V2. *Nature* 421:535-539, 2003.

Xu X, Bosking W, Sáry G, Stefansic J, Shima D, and Casagrande V. Functional organization of visual cortex in the owl monkey. *J Neurosci* 24:6237-6247, 2004.

Yoshioka T and Dow BM. Color, orientation and cytochrome oxidase reactivity in areas V1, V2 and V4 of macaque monkey visual cortex. *Behav Brain Res* 76:71-88, 1996.

Yoshioka T, Dow BM, and Vautin RG. Neuronal mechanisms of color categorization in areas V1, V2 and V4 of macaque monkey visual cortex. *Behav Brain Res* 76:51-70, 1996.

Yoshiyama K, Uka T, Tanaka H, and Fujita I. Architecture of binocular disparity processing in

monkey inferior temporal cortex. *Neurosci Res* 48:155-167, 2004.

Zeki SM. Colour coding in rhesus monkey prestriate cortex. *Brain Res* 53:422-427, 1973.

Zeki S. The representation of colours in the cerebral cortex. *Nature* 284:412-418, 1980.

Zeki S. The distribution of wavelength and orientation selective cells in different areas of monkey visual cortex. *Proc R Soc Lond B Biol Sci* 217:449-470, 1983.

FIGURE LEGENDS

Figure 1

Recording electrode and regions. *A*-*C*: The recording regions in three hemispheres (shaded). Dots indicate the position of the pins inserted so as to verify the recording regions. *D*: Electrode with four recording probes (Tetrode). *E*: A coronal section taken at the level indicated by vertical line in *C*. Dotted line, layer 4. *F*: Photograph of a Nissl-stained section of a portion of area V4 indicated by the box in E. Arrows indicate the two electrolytic lesions made along a recording penetration. The data from this penetration is shown in Figure 15. IV, VI, layers 4 and 6; ls, lunate sulcus; ios, inferior occipital sulcus; sts, superior temporal sulcus. Scale bars, 1 cm in C and E, 500 μm in F.

Figure 2

Visual stimuli. *A*: Stimulus colors plotted on the CIE (Commission Internationale de I'Éclairage)-*xy* chromaticity diagram. The trapezoid indicates the area of CIE coordinates in which our CRT monitor was able to display colors on a luminance plane. *B*: The stimulus colors plotted on the MacLeod-Boynton (M-B) chromaticity diagram. L, M, and S indicate long-, middle- and short-wavelength-sensitive cone signals, respectively.

Figure 3

Example responses of color-selective V4 neurons (*A*-*D*). The peristimulus time histograms (PSTHs) and bubble plots are shown on the CIE (*top row*) and M-B (*bottom row*) chromaticity diagrams. The first vertical dashed line of the PSTHs indicates the appearance of the stationary grating, and the second indicates the start of drifting. The bin width is 40 ms. The CIE chromaticity diagram shows only 18 colors (color numbers 1-12, 16-18, 25-27) to avoid cluttering of PSTHs. The M-B chromaticity diagram represents data for all of the 27 color stimuli. The size of bubbles represents

the magnitude of neuronal responses to the color at each position. The maximal response is indicated by a thick circle (39.6, 16.7, 11.8 and 16.0 imp/s for neurons A-D, respectively). x indicates inhibitory response.

Figure 4

Frequency distribution of color discrimination index (CDI) values for all visually responsive neurons for each of the three monkeys (*A*-*C*) and all the monkeys combined (*D*). Filled bars indicate neurons with color selectivity ($p < 0.05$, Kruskal-Wallis test). The arrows indicate the median of the distribution of CDIs.

Figure 5

A-*C*: Three-dimensional histograms showing the distribution of optimal colors of all color-selective neurons recorded from the three monkeys.

Figure 6

Four examples of color fields of V4 neurons (*A*-*D*). The darkest shading indicates color field that evoked responses greater than 75% of the maximum responses. The second darkest shading was for color field that evoked 50-75% responses, the medium shading for color field that evoked 25-50% responses, and the lightest shading for color field that evoked less than 25% responses. Tilted rectangles indicate the extent of the colors mapped. These example neurons displayed maximum firing rates of 39.6, 17.8, 5.8 and 11.8 (imp/s), respectively. The cells in *A* and *D* are those shown in Figure 2A and 2C, respectively.

Figure 7

Effective color field of a neuron population. Effective color fields for color-selective neurons were superimposed to obtain the effective color field of a neuron population. Shaded areas indicate the region of color space covered by the effective color field of at least one neuron. Degree of shading indicates the number of neurons that occupied corresponding regions.

Figure 8

Correlation of CDI values between neurons simultaneously recorded from single sites. Assignment of a neuron in a pair to either vertical or horizontal axis was arbitrary. Closed circles, open inverted triangles and crosses indicate data from monkey A, B, and C, respectively. Spearman's rank correlation coefficient is shown at the bottom of panel.

Figure 9

Comparisons of color response profiles between nearby neurons simultaneously recorded at single sites. Neuron pairs of positively correlated color preference (*A*, *B*), independent color preference (*C*), negatively correlated color preference (*D*). Bubble plots on the M-B diagram (*left* and *center* panels) and scatter plots (*right* panels) of responses to the 27 colors. All neurons shown were color selective ($p < 0.05$). Spearman's rank correlation coefficients (r) are indicated in the scatter plots. Closed circles: stimuli that evoked significant responses in at least one neuron of the pair. Open circles: ineffective stimuli for both neurons of the pair.

Figure 10

The distribution of color correlation coefficients obtained from color-selective neurons of simultaneously recorded pairs (*A: top panels*) and artificially generated distant pairs (*B: bottom*

panels) in each monkey (*A*-*C*) and all the monkeys (*D*). Filled bars indicate the pairs with a significant correlation. Arrows indicate the median of the distributions of correlation coefficients.

Figure 11

Variation of similarity in color preferences for neuron pairs at individual recording sites. Data were obtained from recording sites where at least three or more neurons had significant color selectivity (Kruskal-Wallis test, $p < 0.05$). *A*-*C*: Correlation coefficients (r) for responses to the 27 color stimuli between all neuron pairs plotted on the order of small SDs to large SDs. Each open circle indicates one neuron pair, and filled diamonds and attached bar indicate the median and ±1 SDs of correlation coefficients for each recording site. *D, E*: Similarity in color preferences at a recording site with a small SD (D, left arrow in *C*) *and* at a recording site with a large SD (E, right arrow in *C*).

Figure 12

Response profiles of V4 neurons recorded at six sites along a vertical penetration. *A*: Histological reconstruction of the electrode track. The reconstructed region was indicated by a box in the inset. Dashed lines indicate borders of layer 4 (IV). sts, superior temporal sulcus. Numbers 1-6, recording sites; IN, the site where we first detected neural activities, WM, entry into white matter. L indicates the location of the electrolytic lesion. Twenty-two visually responsive neurons were recorded along this penetration. *B*: Location of the RF centers at the six recording sites. The RFs of the first and last recording sites are indicated by black and gray circles, respectively. Squares indicate the center of RFs of the other sites. *C*: Response profiles for 17 color-selective neurons ($p < 0.05$, Kruskal-Wallis test) obtained at recording sites 1-6. The optimal colors are indicated by thick circles. The maximum firing rates for each neuron are shown above each panel. *D*: Relation between recording-site distance and color correlation coefficient. Each open circle represents the correlation coefficient between a

pair of color-selective neurons. The filed circle indicates the median of all neuron pairs (pairs in the shaded regions) excluding simultaneously recorded neuron pairs.

Figure 13

Response profiles of V4 neurons recorded in another vertical penetration. *A*: Recording track. Recordings were made at seven sites along this penetration. Unresolved multiple units (MUs) were recorded at site 2, 6, 7. MUs at site 2 were not selective for stimulus colors (NC; $p \geq 0.05$, Kruskal-Wallis test). *B*: RF centers of MUs recorded at sites 1-7. *C*: Responses plotted on the M-B diagrams. *D*: Relation between recording-site distance and color correlation coefficient. Open circles indicate correlation coefficients of neuron pairs at sites 1-4, and open diamonds indicate correlation coefficients of neurons pairs including neurons at sites 5-7. The filed circle and filled diamond indicate the medians of corresponding correlation coefficients for pairs in the shaded regions. Other conventions are the same as in Figure 12.

Figure 14

Relation between the total area of the effective color field of a neuron population and the number of perpendicular penetrations used for calculating population color fields.

Figure 15

Response profiles of V4 neurons recorded in a tangential penetration through upper layers. *A*: Recording track. L1 and L2 indicate the location of electrolytic lesions. Recordings were made at eight sites along this penetration. Unresolved multiple units (MUs) were recorded at site 1-4 and 6-8. MUs at site 1, 3, 6, and 8 were not visually responsive (NR; *t*-test; $p > 0.05$, corrected for multiple comparisons) and MUs at site 7 were not selective for stimulus colors (NC; $p \geq 0.05$, Kruskal-Wallis

test). *B*: Location of the RF centers. *C*: Responses plotted on the M-B diagrams. *D*: Relation between recording-site distance and color correlation coefficient. Other conventions are the same as in Figures 12.

Figure 16

Quantitative summary of the relationship between tangential cortical distance and color correlation coefficient. Each dot indicates one neuron pair. Spearman's rank correlation coefficient is shown at the bottom of panel.

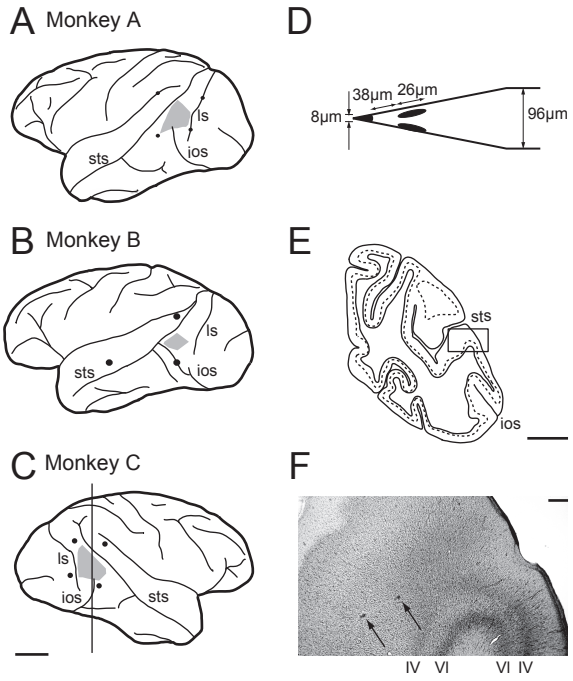

Figure 1. Kotake et al.

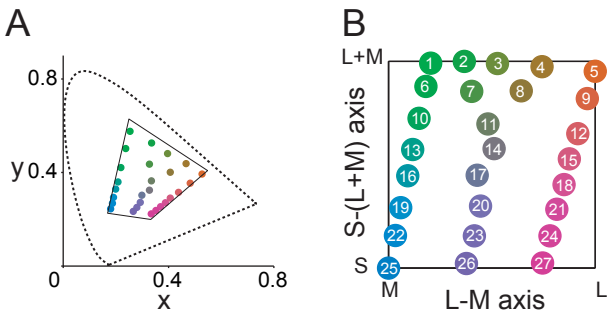

Figure 2. Kotake et al.

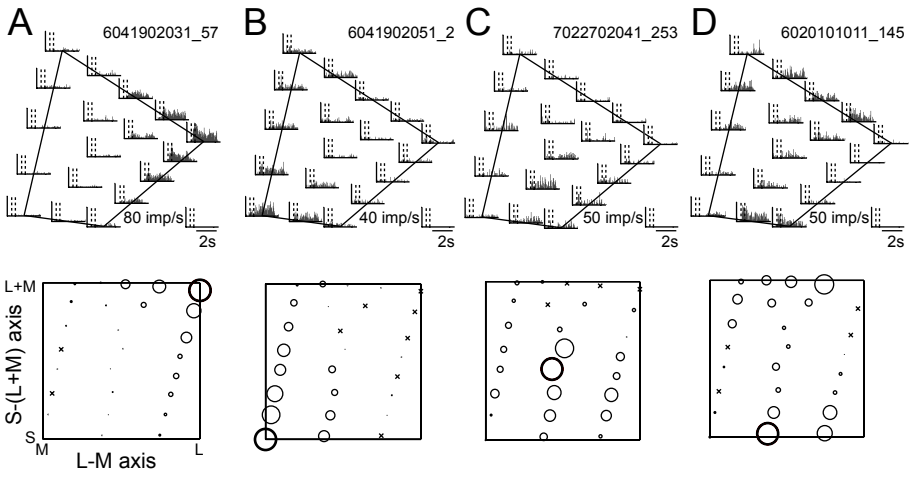

Figure 3 Kotake et al.

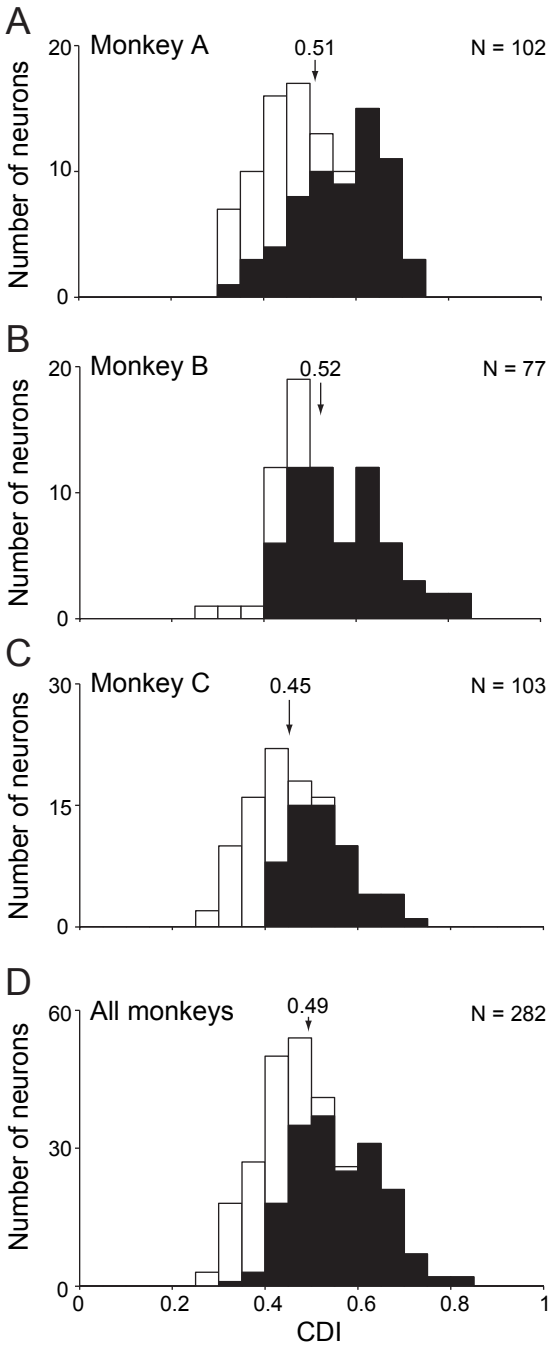

Figure 4 Kotake et al.

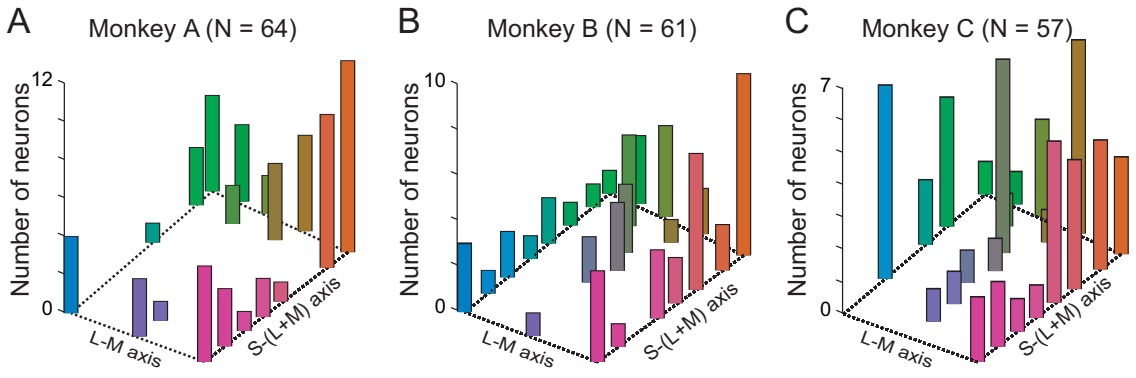

Figure 5. Kotake et al.

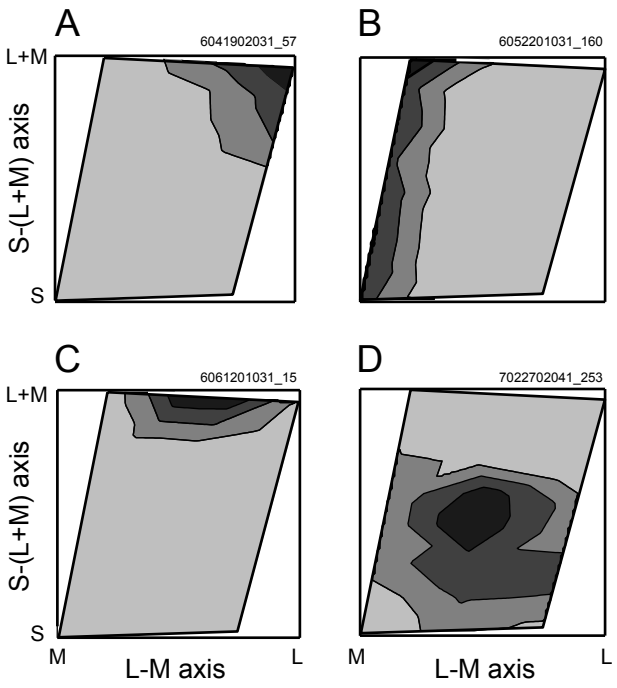

Figure 6. Kotake et al.

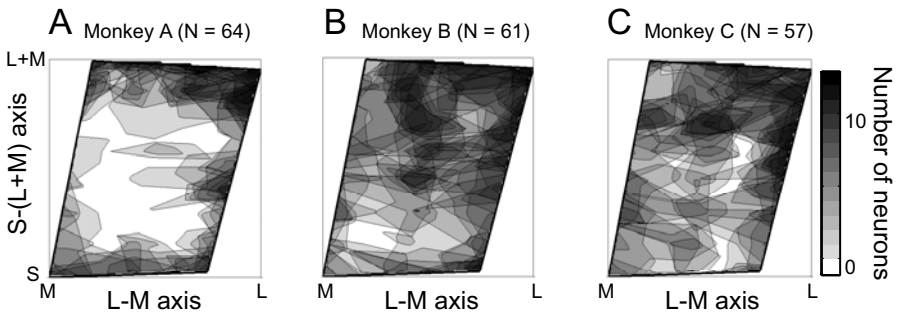

Figure 7 Kotake et al.

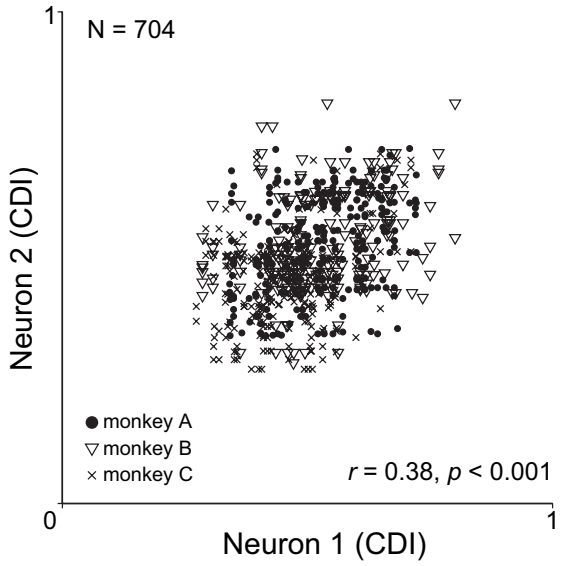

Figure 8 Kotake et al.

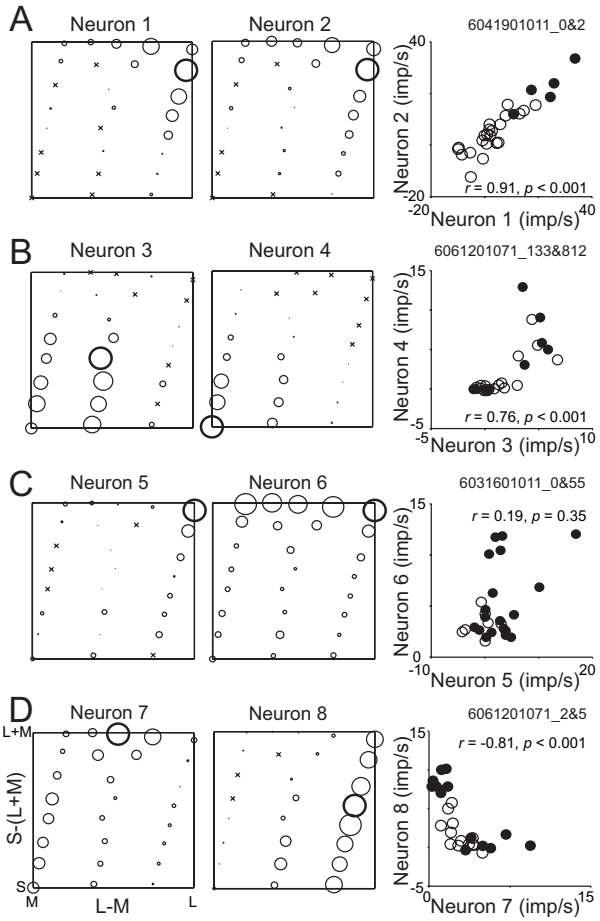

Figure 9. Kotake et al.

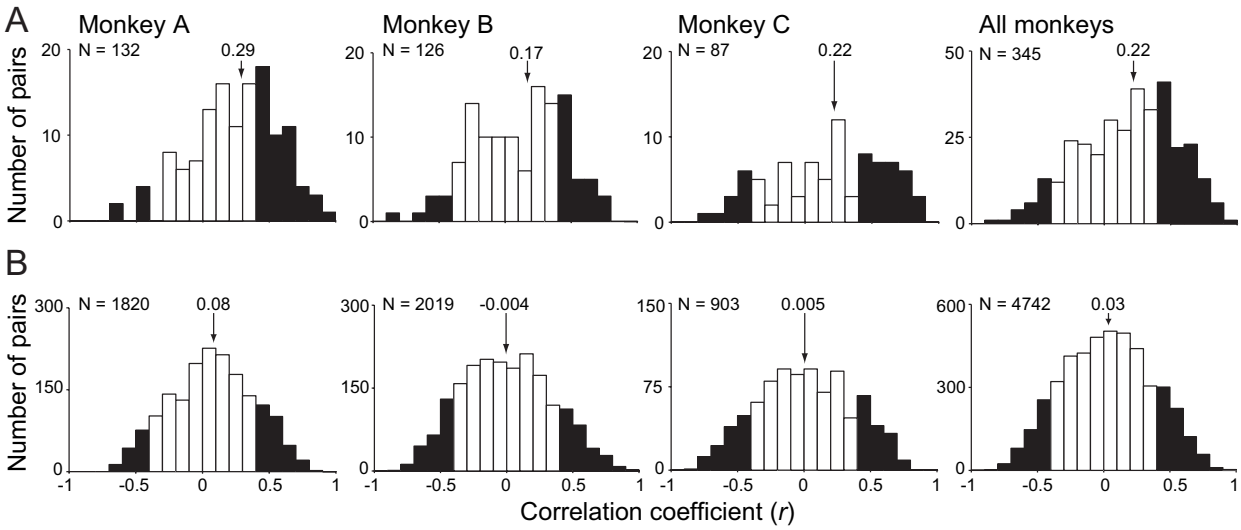

Figure 10. Kotake et al.

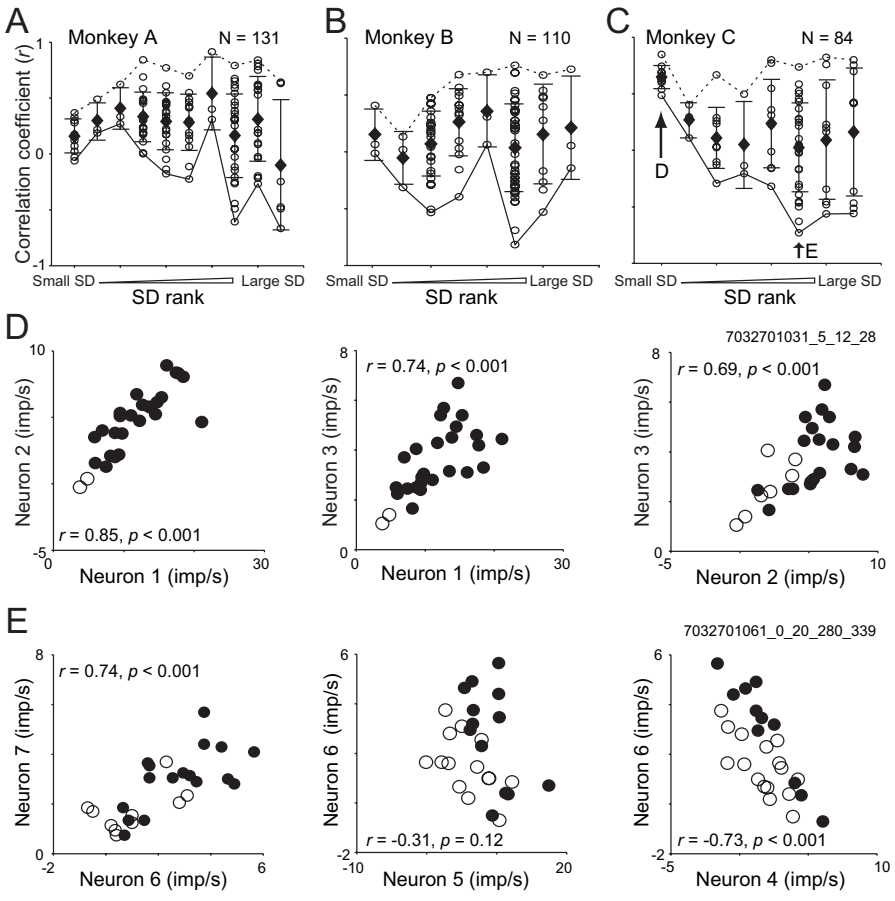

Figure 11 Kotake et al.

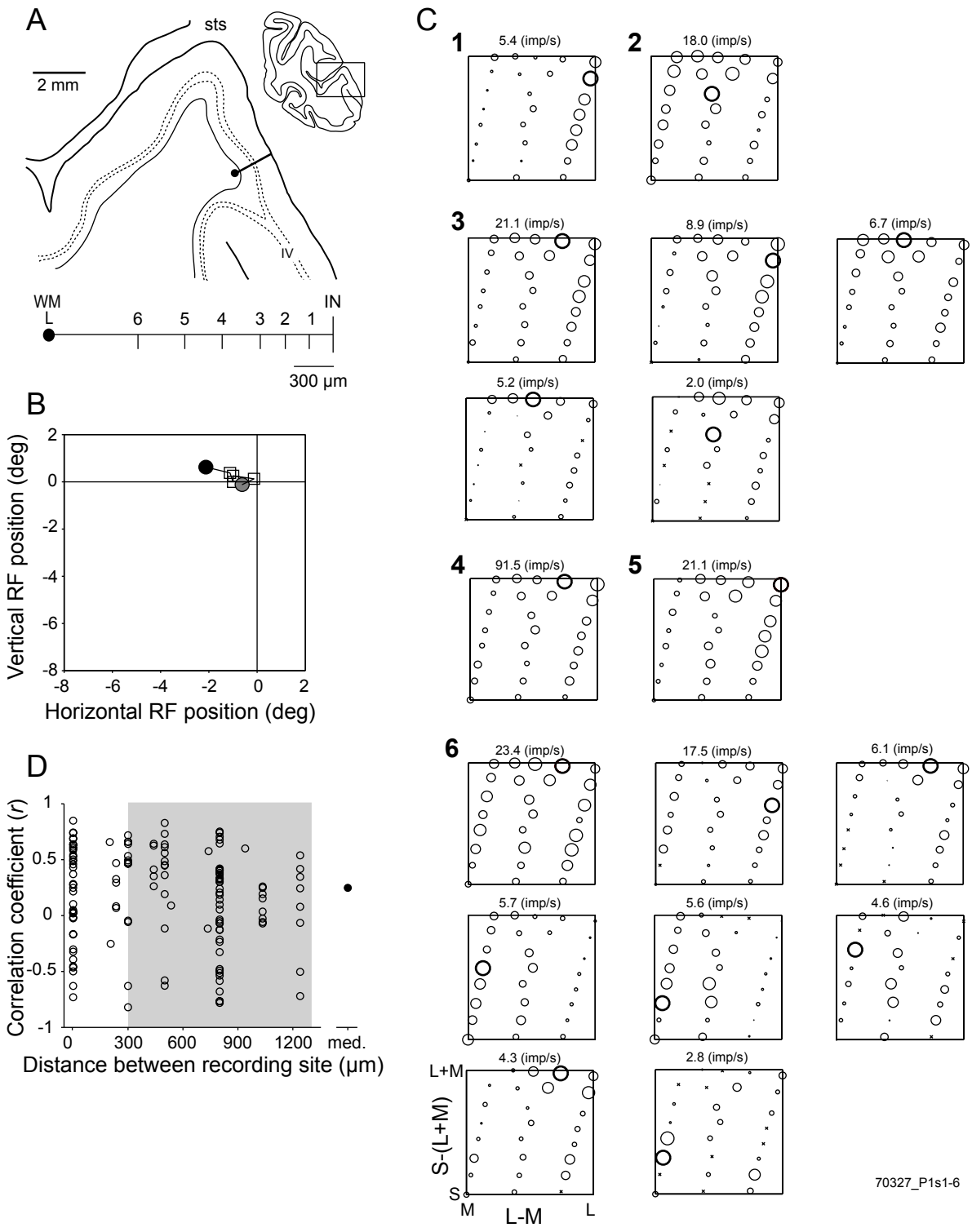

Figure 12. Kotake et al.

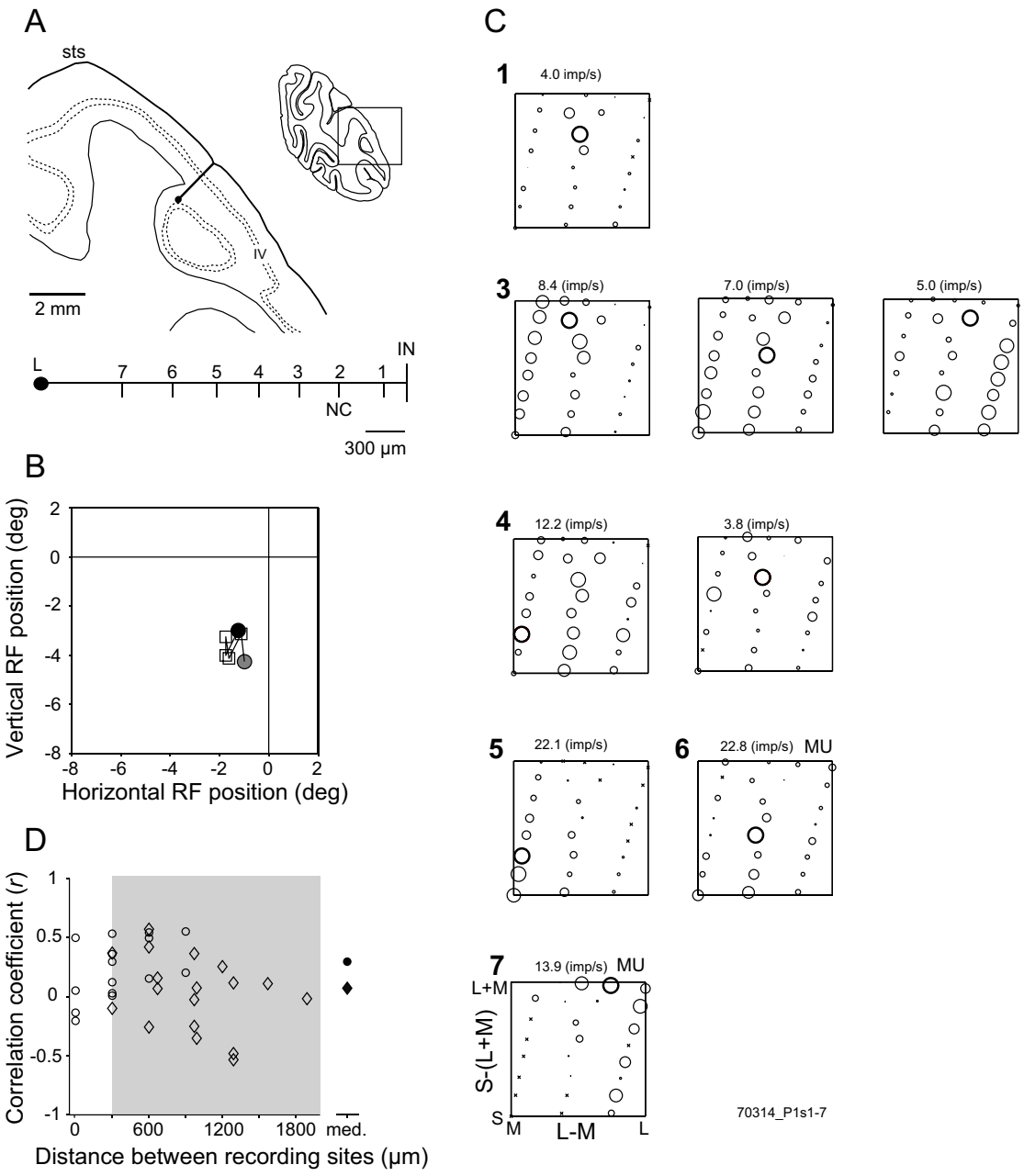

Figure 13. Kotake et al.

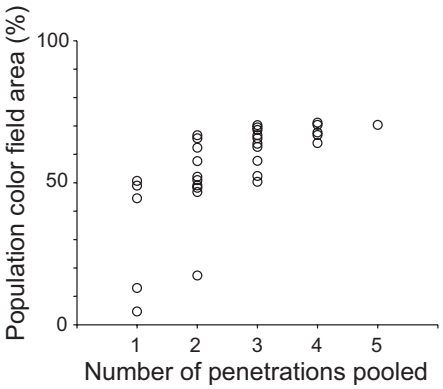

Figure 14. Kotake et al.

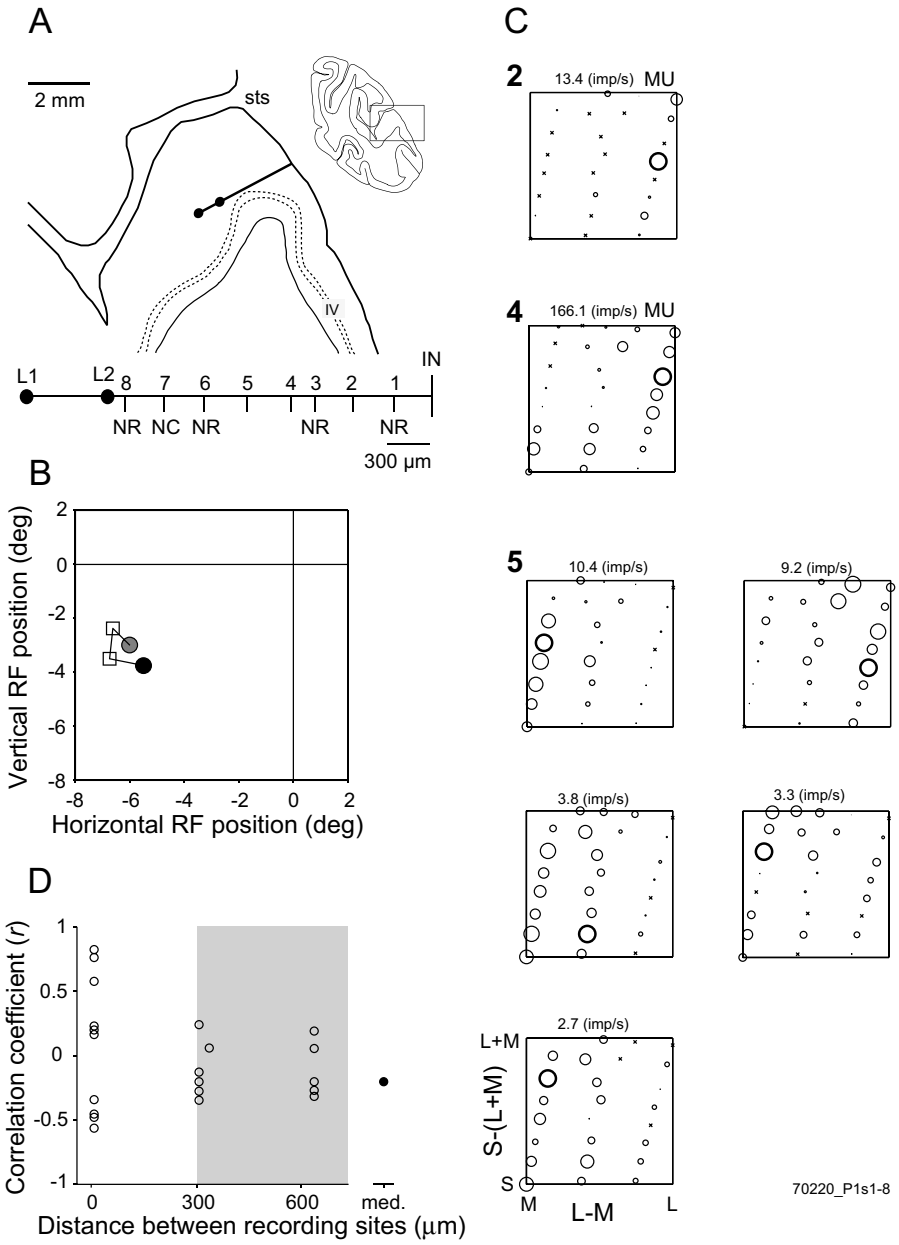

Figure 15. Kotake et al.

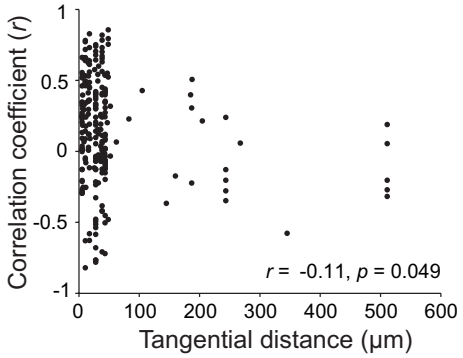

Figure 16. Kotake et al.